

# Phase Separation of L-Menthol an Aqueous Dispersion of Biologically Active Nanoparticles of Chitosan L- and D-Aspartate

**Xenia M. Shipenok<sup>\*</sup>, Aliya M. Mazhikenova, Evgeny G. Glukhovskoy, and Anna B. Shipovskaya**

Saratov National Research State University named after N.G. Chernyshevsky, 83 Astrakhanskaya str.,

Saratov 410012, Russian Federation

<sup>\*</sup>e-mail: [kshipenok@gmail.com](mailto:kshipenok@gmail.com)

**Abstract.** Phase separation in an ethanol solution of L-menthol in an aqueous dispersion of biologically active nanoparticles of chitosan L- and D-aspartate was studied. The process was found to proceed through the mechanism of selective extraction crystallization and to combine two types of phase separation (liquid-liquid and liquid-crystal). Liquid phase separation involves spontaneous dispersion of the ethanol macrophase to form a water microemulsion with hydrophobic content and subsequent coalescence of the dispersed phase. Crystalline phase separation involves L-menthol crystallization into optically anisotropic fibrillar particles. The size of microdroplets and fibrils and their packing density in the condensed phase are significantly affected by the concentration of the components and surface tension of the aqueous macrophase and the enantiomeric form of chitosan aspartate. It has been suggested that the system under study is promising for the development of new approaches to studying the fundamental principles of phase separation during intracellular communication and regulation. © 2024 Journal of Biomedical Photonics & Engineering.

**Keywords:** chitosan; L- and D-aspartic acid; chitosan L- and D-aspartate; nanoparticles; L-menthol; phase separation; extraction crystallization; intracellular regulation; subcellular organization.

Paper #9184 received 23 Oct 2024; revised manuscript received 21 Nov 2024; accepted for publication 25 Nov 2024; published online 14 Dec 2024. [doi: 10.18287/JBPE24.10.040316](https://doi.org/10.18287/JBPE24.10.040316).

## 1 Introduction

Chiral polymeric matrices with controlled sites of complementary-specific interactions are considered as innovative substrates for the production of highly selective medicinal and pharmaceutical drugs [1–3]. To solve this task, first of all, information is necessary about stereospecific features of the chemical substance used to obtain such biomaterials, including those under model conditions of intracellular communication and regulation.

At present, nobody doubts that biochemical reactions inside cells occur in limited spaces of both membraneless and classical membrane organelles – cellular bodies in the form of a drop of liquid (bubble), formed as a result of liquid-liquid phase separation [4–6]). According to the modern concept of phase separation in cell biology,

extracellular vesicles secreted by cells are key participants in intercellular communication and regulation, since they deliver proteins, lipids, nucleic acids and other signaling molecules to recipient cells, ending up in almost all body fluids [7–9]. The component composition of such liquid droplets (bubbles) is not constant and varies depending on the physical or chemical composition of their environment, as well as the local concentrations of low- and high-molecular-weight molecules present therein [10]. Moreover, *in vitro* model experiments have shown that in addition to liquid-liquid phase separation, biomacromolecules may undergo a liquid-crystal phase transition. For example, droplets of RNA-binding proteins may transform into fibrillar structures [11, 12]. The latter are almost stationary, since the exchange rate of the molecular components present therein with the surrounding volume of the solution is

extremely low. The evolution of the liquid–liquid and liquid-crystal transitions *in vitro* is accelerated for mutant variants of these proteins, some of which are known to be pathogenic [12].

An optically active system based on L-menthol and the salt form of chitosan (CS, D-glucan) with L-(D-)aspartic acid (AspA) is considered as a successful model for studying the fundamental principles of intracellular communication and regulation in both physiological and pathological cellular processes [13]. The choice in Ref. [13] of not only L-AspA, a non-essential proteinogenic amino acid [14, 15], but also its D-enantiomer for the production of chitosan aspartate (CS·L-(D-)AspA) is due to an increase in the content of D-AspA in the process of physiological aging of the body due to racemization of L-AspA [16]. The choice of L-menthol is due to its optical and biological activity [17, 18], as well as the diversity of morphostructures and supramolecular symmetries formed when varying the conditions of phase separation: from a water emulsion with hydrophobic content, whose dispersed phase is represented by nano- and microscopic droplets of the hydrophobic component [18, 19], to needle-shaped (whiskers) or lamellar crystals and ring-shaped or non-banded spherulites [13, 20].) Phase separation in an ethanol solution of L-menthol in an aqueous solution of CS·L-(D-)AspA has been established to proceed through the mechanism of extraction crystallization and to combine two types of phase separation, namely: liquid-liquid and liquid-crystal [13]. In the aqueous solution of CS·D-AspA, as well as with an increase in the concentration of the components of the optically active medium, the rate of phase separation, the size of droplets and solid-phase structures increase. It has been suggested that this process mimics the separation of liquid phases during intracellular signal transmission [4, 5].

It was also discovered that the effect of counterionic condensation occurs in the CS + AspA + H<sub>2</sub>O system with phase segregation of the salt form of the polymer substance at the level of nano- and microparticles of CS·L-(D-)AspA [21], whose surface functionalization with a polysiloxane shell ( $\sim\text{Si}-\text{O}-\text{Si}\sim$ ) leads to the production of a kinetically stable aqueous dispersion of CS·L-(D-)AspA·Si particles [22]. It has been established that CS·L-(D-)AspA and CS·L-(D-)AspA·Si nanoparticles are non-toxic, hemo- and biocompatible, and also exhibit a bactericidal action against *Staphylococcus aureus* 209 P and *Escherichia coli* 113-13 with the best effect for homochiral particles of D-glucan·D-AspA [22, 23]. It seems to us that a dispersion of CS·L-(D-)AspA·Si nanoparticles, like CS·L-(D-)AspA solutions, could be a promising model for studying the colloidal phase separation of biologically active substances.

The purpose of this work was to study features of crystallization of the L-menthol + ethanol system in an aqueous dispersion of CS·L-(D-)AspA·Si nanoparticles.

## 2 Materials and Methods

### 2.1 Materials

The following reagents were used: CS with a viscosity-average molecular weight of 200 kDa, a degree of deacetylation DD of 82 mol % (Bioprogress Ltd., RF), L-AspA (JSC Bioamid, RF); D-AspA (Vekton Ltd., RF), laboratory-synthesized silicon tetraglycolate (Si(OGly)<sub>4</sub>) obtained via the method described elsewhere [24], L-menthol with 99% basic substance (Alfa Aesar, Heysham, Lancs, UK), 95% ethyl alcohol (RFK Corp., Orel, RF), and distilled water. All reagents were chemical grade and used without further purification.

### 2.2 Preparation of Solutions and Nanoparticles

To obtain L-(D-)AspA solutions with a concentration of 0.3 g/dL, weighed portions of L- and D-AspA powders were dissolved in distilled water with stirring on a Labdevices HMS-100D heating mantle (China) at 80 °C, followed by cooling down to room temperature at 20 °C/h.

To prepare CS·L-(D-)AspA solutions, weighed portions of CS, L- or D-AspA powders were dissolved in distilled water with stirring in an Atlas reactor (Syrris, England) for 3 h at 50 °C. The concentrations of CS ( $C_{\text{CS}}$ ), L- and D-AspA ( $C_{\text{AspA}}$ ) were varied in a range of 0.3–1.2 g/dL, maintaining the molar ratio  $[\text{Asp}]/[\text{CS}]$  at  $1.3 \text{ mol} \cdot (\text{mol of NH}_2)^{-1}$ . CS·L-(D-)AspA solutions were filtered through a Schott-160 funnel, Si(OGly)<sub>4</sub> was added thereto at a rate of  $\sim 0.08 \text{ g}$  of precursor per 25 mL of solution, and stirred at 50 °C for 6 h, as described above. As a result, an aggregation and sedimentation stable dispersion of CS·L-(D-)AspA·Si nanoparticles was formed. A detailed procedure for functionalizing the surface of particles is given in Ref. [22].

A solution of L-menthol with a concentration of 2.5 g/dL was prepared by dissolving a sample of air-dry L-menthol in 95% ethyl alcohol for 24 h.

### 2.3 Methods

Gravimetric measurements were carried out on an Ohaus Discovery analytical balance (USA), weighing accuracy being  $\pm 0.01 \text{ mg}$ .

To explore the phase separation, 3 ml of an aqueous dispersion of CS·L-(D-)AspA·Si was poured into a Petri dish 4 cm in diameter, and 1.5 ml of an ethanolic L-menthol solution was added dropwise onto the surface of the liquid medium with an automatic dispenser without stirring. The Petri dish was covered with a cover glass and left under static conditions in an air atmosphere at a temperature of  $23 \pm 1^\circ\text{C}$  for 48 h. The phase separation process was considered complete if there were no changes in the morphostructure of the condensed phase.

The phase separation was observed both visually and on a LaboPol-2 (RF) polarization microscope (PM) with the polarizer and analyzer crossed. A halogen lamp (12 V, 30 W) served as the light source. The microscope

was focused on the site of space located at the Petri dish's center. PM-photos were obtained by a DMC 300 (3 Mpx) USB camera (Hangzhou, China). Temperature was measured using a mercury thermometer TL-5-2 (RF) with a measurement range of 0–105 °C and a division value of 0.5 °C.

Interfacial surface tension ( $\sigma$ , mN/m) was measured by the Wilhelmy plate lift-off method at the liquid-gas (air) interface at  $24 \pm 2$  °C, the accuracy being 0.1 mN/m. Distilled water was used to calibrate the Wilhelmy balance. Three replicate experiments with 10 measurements each were carried out. When calculating  $\sigma$  values, a correction was introduced for the temperature coefficient of the surface tension of water [25].

Contact angles ( $\theta$ , deg) were measured by the sessile drop method at the solid-liquid-gas interface on an Attension Theta Lite TL 100 precision optical tensiometer from Biolin Scientific (Sweden), the accuracy was 0.1 deg. An optical-quality glass slide, previously cleaned of contaminants, was used as a substrate, and distilled water was used as the base liquid. The time it took for a drop of liquid on the glass substrate to reach equilibrium was 25 s.

### 3 Results and Discussion

After applying the ethanol solution of L-menthol onto the surface of the aqueous dispersion of CS·L-(D-)AspA·Si nanoparticles, almost immediately there was a sharp increase in the temperature of the aqueous macrophase by 3–5 °C (depending on  $C_{CS}$  and  $C_{AspA}$ ), the release of vaporous products and their condensation in volume to form a whitish fog. Fig. 1 (a–d) shows typical photos of this phenomenon when the dispersion of CS·D-AspA·Si nanoparticles is used as the aqueous phase. In parallel, turbulent movement of the liquid begins throughout the entire bulk of the ethanol macrophase and its spontaneous dispersion in the aqueous macrophase with the formation of a direct water microemulsion with hydrophobic content (Table 1,  $t = 0.02$  h). Note that no increase in

temperature, no formation of a dynamic aerosol cloud and no intense movement of ethanol layers occur if solutions of individual L-(D-)AspA and solutions of CS·L-(D-)AspA salts studied by us earlier [13] are used as the aqueous phase.

When a glass plate stored in a room atmosphere at  $23 \pm 1$  °C is introduced into the space of the aerosol cloud, droplets of ovoid-shaped condensate appear on its surface, which quickly take a spherical shape and evaporate (Fig. 1 (e–g)).

Subsequently, a coalescence process of microdroplets proceeds due to Brownian aggregation of particles (Table 1,  $t = 0.5$  h) and crystallization of an optically active low-molecular-weight substance into anisodiametric (fibrillar) solid-phase particles with pronounced optical anisotropy ( $t = 24$ –48 h). In addition, Janus-like objects (supramolecular structures with signs of Janus particles) are observed, especially at  $t = 48$  h. At  $t = 48$  h, some attenuation of the condensed phase birefringence was observed, but the effect of optical anisotropy did not completely disappear. With increasing concentrations of CS and L-(D-)AspA in the initial solution used to obtain nanoparticles, the size of spontaneously formed droplets in the liquid macrophase of the antisolvent and the length/thickness of solid-phase fibrils increase.

In the medium of individual enantiomers of L- and D-AspA, as well as in that of CS·L-(D-)AspA·Si, two types of phase separation are also observed: liquid-liquid and liquid-crystal (Table 1). However, the size of phase-separated microdroplets is significantly smaller (submicron size), the onset time of coalescence of emulsion droplets increases up to 5–6 h, and the condensed phase is mainly represented by optically isotropic needle-like crystals (thread-like whiskers) and their aggregates. A similar type of solid-phase particles was observed during the crystallization of L-menthol in the CS·L-(D-)AspA medium [13].

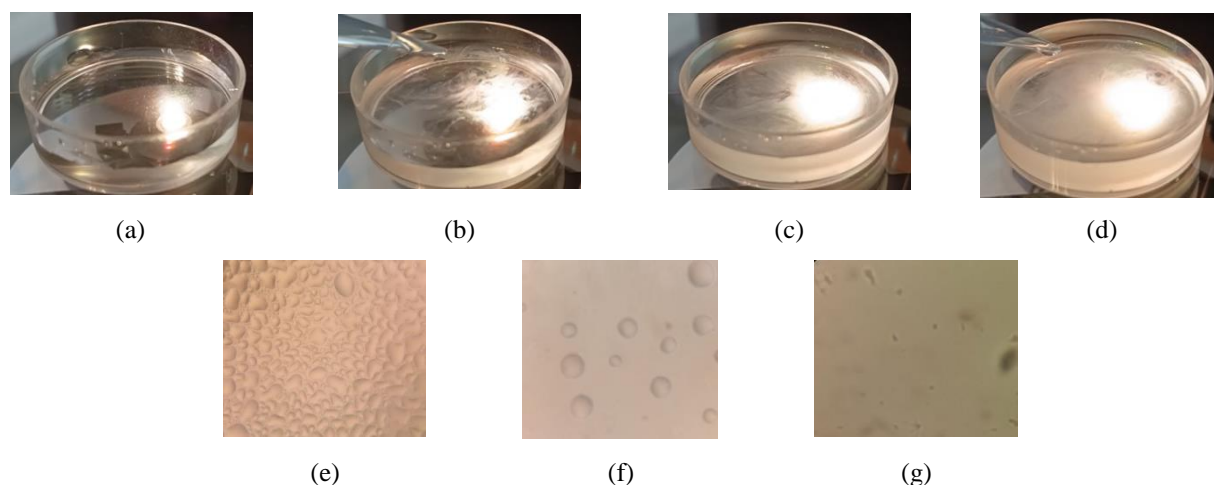
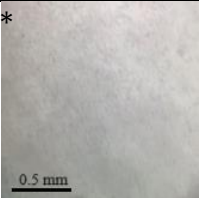
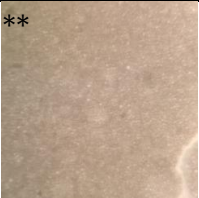
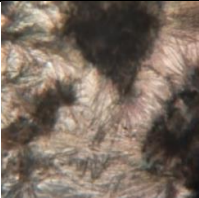

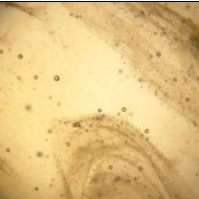

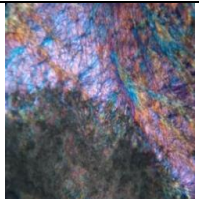
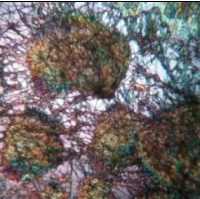

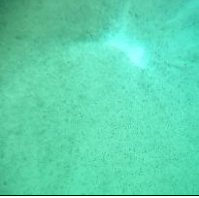
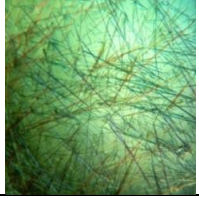
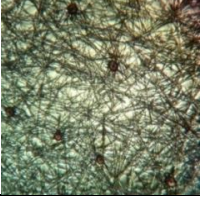

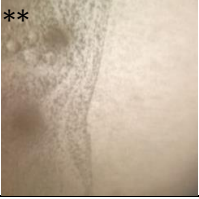
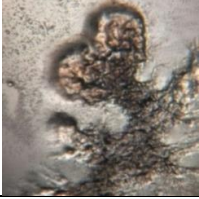
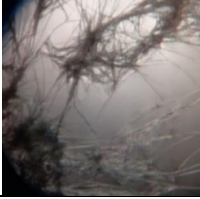
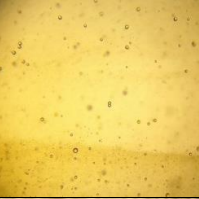

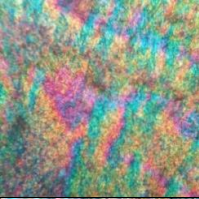
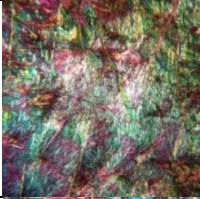
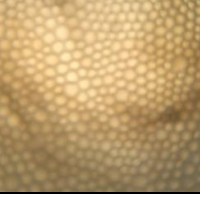
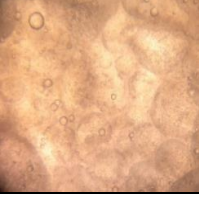
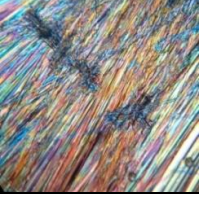
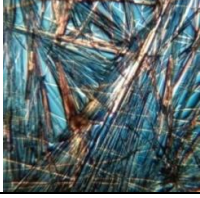


Fig. 1 Photos: Petri dishes (a) with the initial dispersion of CS·D-AspA·Si nanoparticles and the initial stage of applying the ethanol solution of L-menthol onto its surface at a contact time ( $t$ ) between the ethanol and aqueous macrophases of (b) 4, (c) 10 and (d) 20 s; condensate of the aerosol cloud shown in panel (d) on the surface of a glass plate at (e)  $t = 0.02$ , (f) 0.05 and (g) 4 h; the concentration of aqueous phase components  $C_{CS} = 1.2$  g/dL,  $C_{AspA} = 1.2$  g/dL.

Table 1 Photos of the stages of extraction crystallization of the ethanol solution of L-menthol in the aqueous solutions of L-(D-)AspA and aqueous dispersions of CS·L-(D-)AspA·Si nanoparticles, magnification ×4.

Concentration of aqueous phase components		PM-photos of forming droplets, fibrillar structures and their supramolecular aggregates			
		Contact time <i>t</i> , h			
<i>C</i> <sub>CS</sub> , g/dL	<i>C</i> <sub>AspA</sub> , g/dL	0.02	0.5	24	48
L-AspA					
—	0.3	<div><div>*</div></div>	<div><div>**</div></div>		
CS·L-AspA·Si					
0.3	0.3				
1.2	1.2				
D-AspA					
—	0.3	<div><div>*</div></div>	<div><div>**</div></div>		
CS·D-AspA·Si					
0.3	0.3				
1.2	1.2				

\*, \*\* Time – 0.08 and 6 h, respectively.

But the whiskers were ordered into optically anisotropic non-banded spherulites, and upon transition to the air-dry state they formed needle-shaped spherulites of a “leaked radial configuration” with macroscopic chirality.

Crystallization in droplets with the formation of spherulites was not observed in the CS·L-(D-)AspA·Si medium, which is probably due to the functionalization of nanoparticles with a polysiloxane shell.



Our assessment of the influence of the AspA isomer on the observed processes showed that the rate of increase in the temperature of the aqueous macrophase when a hydrophobic weakly polar macrophase is applied onto its surface was greater when carrying out the phase separation of L-menthol in the CS·D-AspA·Si medium. In the same environment, the resulting fog was whiter, and the emulsion droplets were larger and more uniform in size. The length/thickness of the fibrils and the packing density of their supramolecular aggregates were greater than for similar structures upon crystallization in CS·L-AspA·Si. In the liquid phase of AspA enantiomers, on the contrary, the densest condensed phase was formed in the L-AspA medium. The birefringence effect was most pronounced for fibrils condensed in the CS·D-AspA·Si phase.

One of the causes for the observed nature of phase separation of an ethanol solution of L-menthol in an aqueous dispersion of CS·L-(D-)AspA·Si may be some specificity of the structural and molecular ordering of the aqueous macrophase, determined by its surface energy. Recent studies [26] have shown that in terms of surface activity, nanoparticles in dispersions behave in many ways similar to surfactant molecules, with the only difference being that the orientation of nanoparticles (especially spherical ones) relative to the surface has virtually no effect on the interfacial tension, and the adsorption energy of nanoparticles on the surface changes sharply with the wetting angle. In this regard, the surface tension and contact angle of the CS·L-(D-)AspA·Si + H<sub>2</sub>O system were estimated.

It turned out that chitosan L-(D-)aspartate nanoparticles had surface activity and reduced the surface energy at the liquid-gas interface. At the same time, the interfacial tension of the aqueous dispersion of CS·L-AspA·Si and CS·D-AspA·Si nanoparticles non-monotonically decreases with increasing  $C_{CS}$ , and is also significantly lower than the interfacial tension of the base liquids-water, an aqueous solution of the surface-inactive L-aspartic acid and an aqueous solution of CS L-AspA (Fig. 2(a)). Probably, the compacted conformation of macrocoils in the structure of CS·L-(D-)AspA·Si nanoparticles weakens the intermolecular interactions of the components in the bulk of the aqueous macrophase and, as a result, reduces the surface adsorption energy and surface tension. The synergistic effect of increasing surface activity was more pronounced in the aqueous macrophase with CS·L-AspA·Si nanoparticles.

The formation of a drop of an aqueous dispersion of CS·L-(D-)AspA·Si nanoparticles on glass occurs in the limited wetting mode (Fig. 2(b)). The surface of the glass substrate is more lyophilic for the CS·L-AspA·Si dispersion, which explains its higher surface activity at the liquid-gas interface in comparison with CS·D-AspA·Si. At the same time, the contact angle at the solid-liquid-gas interface monotonically increases with CS concentration. Therefore, the interactions between the components of the aqueous macrophase become more preferable than the interactions of these same

components with the substrate surface. This character of the  $\theta = f(C_{CS})$  dependence is expressed to the greatest extent for the dispersion of CS·D-AspA·Si nanoparticles. One more discovered nontrivial effect should also be noted. Despite the fact that the  $\sigma$  of aqueous dispersions of both isomeric forms of chitosan aspartate nanoparticles is less than that of water, the contact angle of the aqueous dispersion of CS·D-AspA·Si is greater than that of water on the same glass substrate.

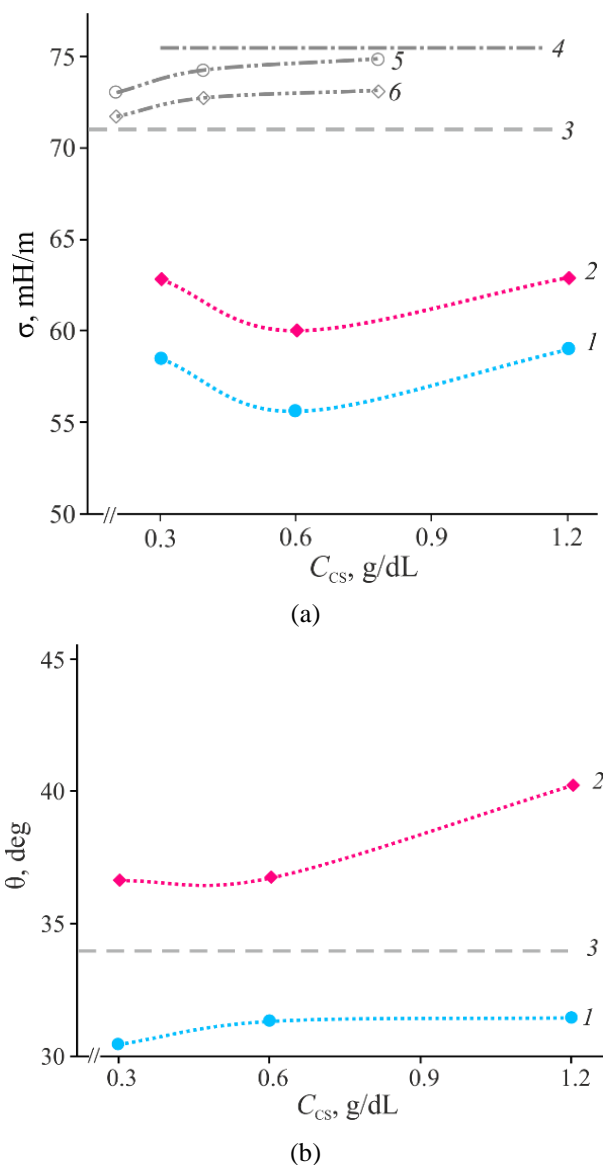


Fig. 2 (a) Surface tension and (b) contact angle of an aqueous dispersion of (1) CS·L-AspA·Si and (2) CS·D-AspA·Si nanoparticles as a function of CS concentration. The dotted line (3) in panels (a) and (b) shows the  $\sigma$  and  $\theta$  values for distilled water. The dashed-dotted line (4) in panel (a) corresponds to the  $\sigma$  values of aqueous solutions of L-AspA with concentrations between 0.3–1.2 g/dL, according to Ref. [27] and the dashed-dotted curves (5) and (6) corresponds to the  $\sigma$  values of aqueous solutions of L-AspA and D-AspA, respectively, with concentrations between 0.2–0.8 g/dL.

## 4 Conclusion

The phase separation of an ethanolic L-menthol solution in an aqueous CS·L-(D-)AspA dispersion proceeds through the mechanism of selective extraction crystallization and combines two types of phase separation (liquid-liquid and liquid-crystal). At the initial stage of liquid-phase separation, the interaction of the ethanol solution of L-menthol with the aqueous dispersion of chitosan nanoparticles to spontaneously form hydrophobic droplets turns out to be the most preferable. During liquid–solid phase separation, the preferred morphostructural organization of L-menthol is optically anisotropic fibrillar particles. The formation of Janus-like objects also indicates spontaneous (controlled) phase separation. The size of microdroplets and fibrils and their packing density in the condensed phase are significantly affected by the concentration of the components of the aqueous macrophase and the enantiomeric form of chitosan aspartate. The surface properties of the initial dispersion of CS·L-(D-)AspA·Si nanoparticles have an important effect on the specific nature of phase separation in the studied system. In comparison with the base liquid (H<sub>2</sub>O), the presence of

nanoparticles in the aqueous phase not only increases surface adsorption at the liquid–gas interface, but also specifically changes the lyophilic balance of the nanodispersion components at the solid-liquid-gas interface.

The results obtained show the promise of using CS·L-(D-)AspA·Si nanoparticles in studies of biomolecular condensation and the biogenesis of membraneless/membrane organelles in physiological/pathological cellular processes and, accordingly, the development of new pharmaceutical compositions to treat specific diseases.

## Acknowledgements

This research was funded by a grant from the Russian Science Foundation No. 24-16-00172, <https://rscf.ru/project/24-16-00172/>.

## Disclosures

All authors declare that there is no conflict of interests in this paper.

## References

1. H. Zhong, J. Deng “Organic polymer-constructed chiral particles: preparation and chiral applications,” *Polymer Reviews* 62(4), 826–859 (2022).
2. L. Song, M. Pan, R. Zhao, J. Deng, and Y. Wu, “Recent advances, challenges and perspectives in enantioselective release,” *Journal of Controlled Release* 324, 156–171 (2020).
3. H. Yu, X. Yong, J. Liang, J. Deng, and Y. Wu, “Materials established for enantioselective release of chiral compounds,” *Industrial and Engineering Chemistry Research* 55(21), 6037–6048 (2016).
4. S. V. Nesterov, N. S. Ilyinsky, and V. N. Uversky, “Liquid-liquid phase separation as a common organizing principle of intracellular space and biomembranes providing dynamic adaptive responses,” *Biochimica et Biophysica Acta - Molecular Cell Research* 1868(11), 119102 (2021).
5. D. M. Mitrea, R. W. Kriwacki, “Phase separation in biology; functional organization of a higher order,” *Cell Communication and Signaling* 14(1), 1 (2016).
6. M. Feric, N. Vaidya, T. S. Harmon, D. M. Mitrea, L. Zhu, T. M. Richardson, R. W. Kriwacki, R. V. Pappu, and C. P. Brangwynne, “Coexisting liquid phases underlie nucleolar subcompartments,” *Cell* 165(7), 1686–1697 (2016).
7. P. Robbins, A. Morelli, “Regulation of immune responses by extracellular vesicles,” *Nature Reviews Immunology* 14, 195–208 (2014).
8. A. C. Dixon, T. R. Dawson, and D. Di Vizio, “Context-specific regulation of extracellular vesicle biogenesis and cargo selection,” *Nature Reviews Molecular Cell Biology* 24, 454–476 (2023).
9. L. P. Bergeron-Sandoval, N. Safaei, and S. W. Michnick, “Mechanisms and consequences of macromolecular phase separation,” *Cell* 165(5), 1067–1079 (2016).
10. L. Zhu, C. P. Brangwynne, “Nuclear bodies: the emerging biophysics of nucleoplasmic phases,” *Current Opinion in Cell Biology* 34, 23–30 (2015).
11. A. Molliex, J. Temirov, J. Lee, M. Coughlin, A. P. Kanagaraj, H. J. Kim, T. Mittag, and J. P. Taylor, “Phase separation by low complexity domains promotes stress granule assembly and drives pathological fibrillization,” *Cell* 163(1), 123–133 (2015).
12. Y. Lin, D. S. W. Protter, M. K. Rosen, and R. Parker, “Formation and maturation of phase-separated liquid droplets by RNA-binding proteins,” *Molecular Cell* 60(2), 208–219 (2015).
13. A. B. Shipovskaya, N. O. Gegel, and X. M. Shipenok, “Features of L-menthol crystallization in optically active medium based on L- and D-asparaginate chitosan features of L-menthol crystallization in optically active medium based on L- and D-asparaginate chitosan,” *Journal of Biomedical Photonics* 9(1), 010305 (2023).
14. N. J. Ayon, “Features, roles and chiral analyses of proteinogenic amino acids,” *AIMS Molecular Science* 7(3), 229–268 (2020).
15. L. Tu, Y. K. Lin, “The origin of life and the crystallization of aspartic acid in water,” *Crystal Growth and Design* 10(4), 1652–1660 (2010).

16. A. V. Chervyakov, N. V. Gulyaeva, and M. N. Zakharova, “[D-Amino acids in normal ageing and pathogenesis of neurodegenerative diseases](#),” *Neurochemical Journal* 5(2), 100–114 (2011).
17. A. G. Shtukenberg, Y. O. Punin, A. Gujral, and B. Kahr, “[Growth actuated bending and twisting of single crystals](#),” *Angewandte Chemie International Edition* 53(3), 672–699 (2014).
18. E. Betz-Güttner, M. Righi, S. Micera, and A. Fraleoni-Morgera, “[Directional growth of cm-long PLGA nanofibers by a simple and fast wet-processing method](#),” *Materials* 15(2), 687 (2022).
19. S. Kim, S. C. Peterson, “[Optimal conditions for the encapsulation of menthol into zein nanoparticles](#),” *LWT* 144, 111213 (2021).
20. T. Kovács, R. Szűcs, G. Holló, Z. Zuba, J. Molnár, H. K. Christenson, and I. Lagzi, “[Self-assembly of chiral menthol molecules from a liquid film into ring-banded spherulites](#),” *Crystal Growth and Design* 19(7), 4063–4069 (2019).
21. T. N. Lugovitskaya, A. B. Shipovskaya, S. L. Shmakov, and X. M. Shipenok, “[Formation, structure, properties of chitosan aspartate and metastable state of its solutions for obtaining nanoparticles](#),” *Carbohydrate Polymers* 277, 118773 (2022).
22. A. Shipovskaya, X. Shipenok, T. Lugovitskaya, and T. Babicheva, “[Self-assembling nano- and microparticles of chitosan L-and D-aspartate: preparation, structure, and biological activity](#),” *Materials Proceedings* 14(1), 31 (2023).
23. A. B. Shipovskaya, T. N. Lugovitskaya, and I. V. Zudina, “[Biocidal activity of chitosan aspartate nanoparticles](#),” *Microbiology* 92(1), 75–82 (2023).
24. E. V. Shadrina, O. N. Malinkina, T. G. Khonina, A. B. Shipovskaya, V. I. Fomina, E. Yu. Larchenko, N. A. Popova, I. G. Zyryanova, and L. P. Larionov, “[Formation and pharmacological activity of silicon—chitosan-containing glycerohydrogels obtained by biomimetic mineralization](#),” *Russian Chemical Bulletin* 64, 1633–1639 (2015).
25. G. Kaptay, “[On the temperature dependence of surface tension: Historical perspective on the Eötvös equation of capillarity, celebrating his 175th anniversary](#),” *Advances in Colloid and Interface Science* 332, 103275 (2024).
26. A. M. Emelianenko, and L. B. Boinovich, “[Role of disperger particles in physical-chemical movement of nanofluids](#),” *Colloid Journal* 85(6), 727–737 (2023).
27. T. N. Lugovitskaya, and A.B. Shipovskaya “[Physicochemical properties of aqueous solutions of L-aspartic acid containing chitosan](#),” *Russian Journal of General Chemistry* 87(4), 782–787 (2017).